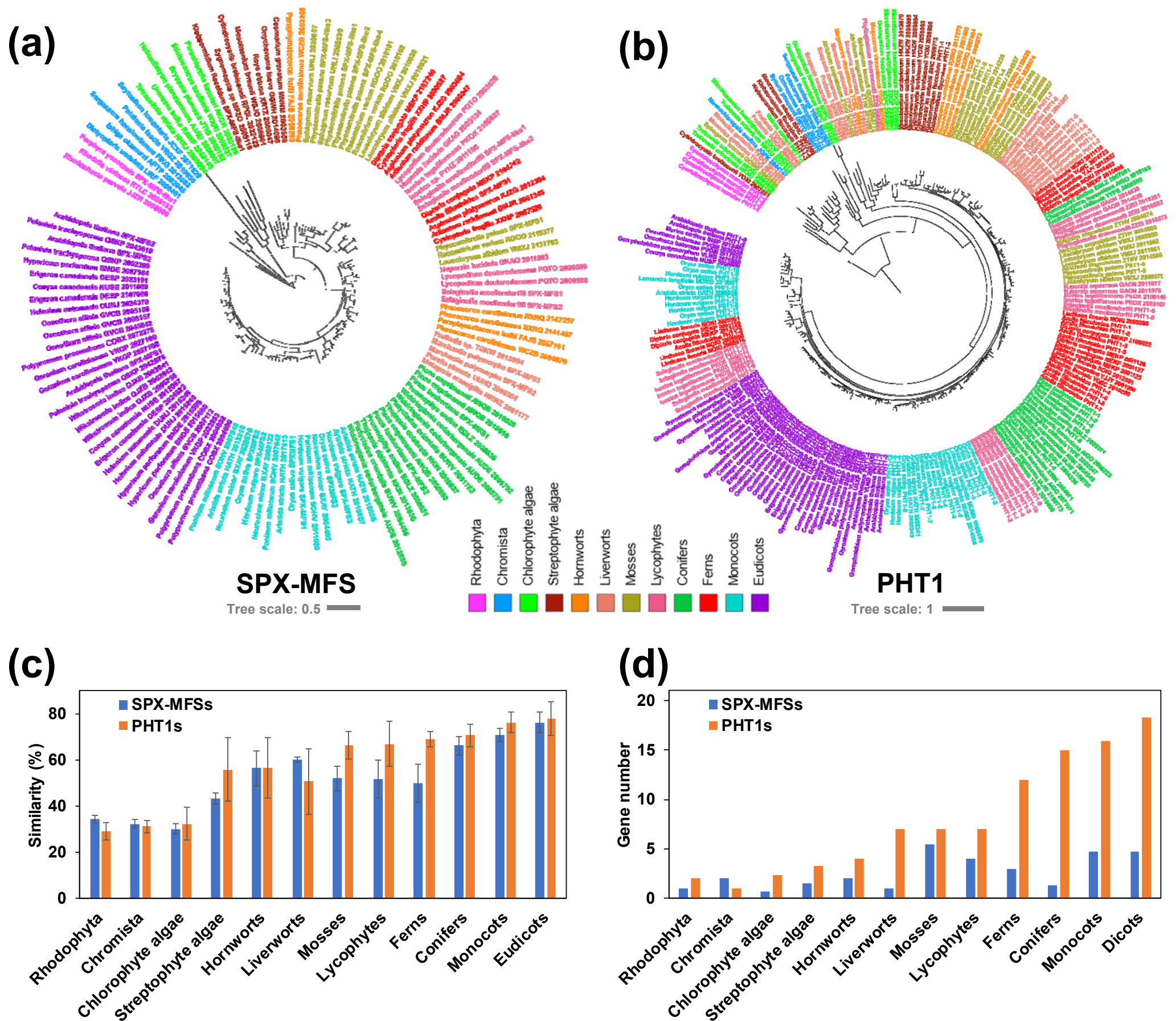
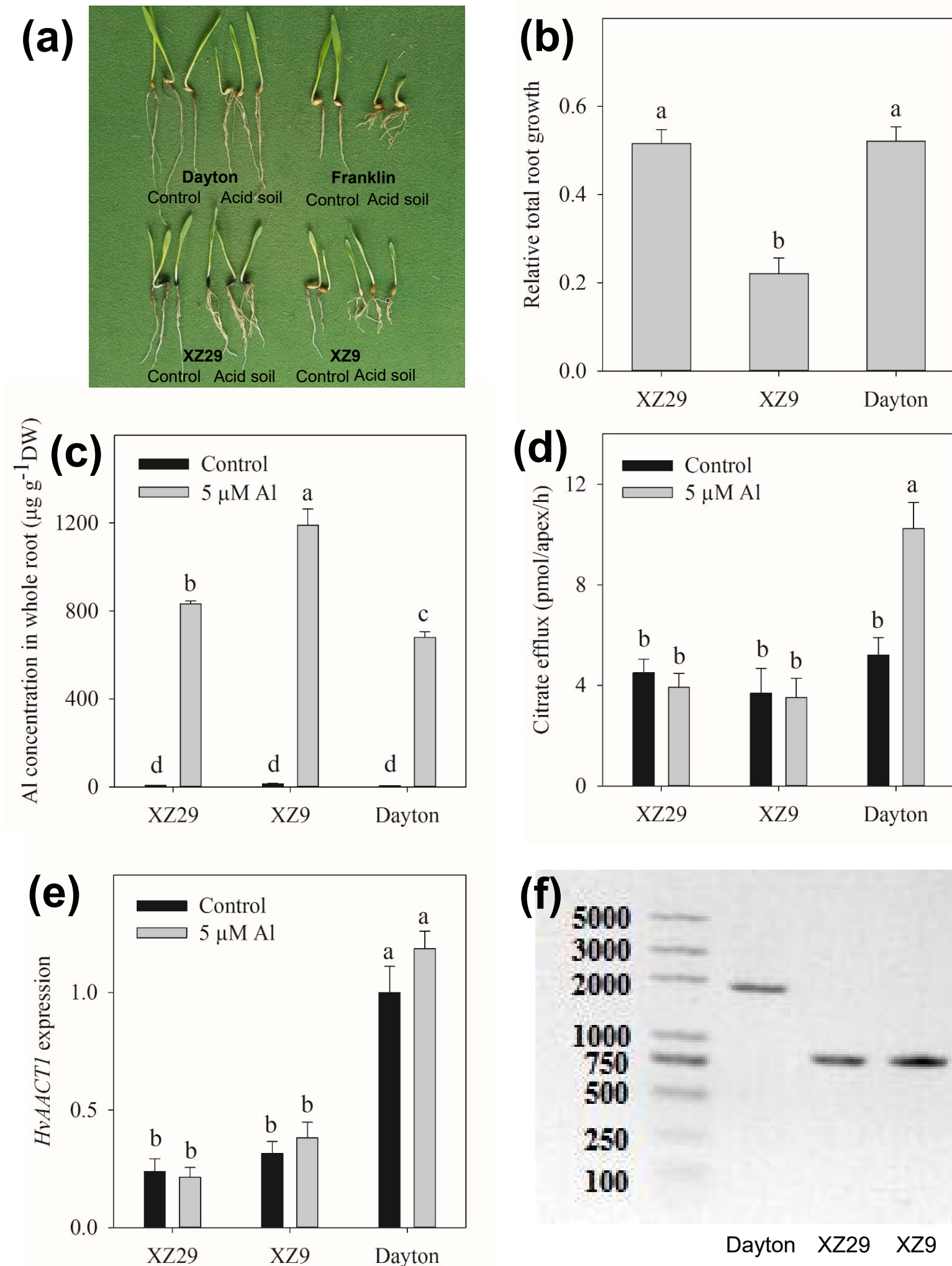


**Figure 1.** Similarity heatmap of protein sequences of Al tolerance-associated genes/ gene families in 41 land plants and algae. The detailed information of these gene family was shown in Table S2. Colored squares indicate protein sequence similarity from zero (yellow) to 100% (red) and gray indicates no match of sequences in this species.



**Figure 2.** Phylogenetic analysis of SPX-MFSs and PHT1s from algae to angiosperms. (a,b) Phylogenetic tree of SPX-MFSs (a) and PHT1s (b). (c) Average protein similarity of SPX-MFSs and PHT1s in different plant clades. (d) Average gene number of SPX-MFSs and PHT1s in different plant clades. The protein sequences were obtained from OneKP database and published genome database. The protein sequences were aligned using MAFFT, and the conserved domains were generated using Gblocks software, and the maximum likelihood (ML) tree was constructed using FastTree and was displayed using iTOL.



**Figure 3.** Effect of Al on root growth, Al concentration, citrate secretion and *HvAACT1* gene expression. (A) Images of seven-day-old seedlings of XZ29, XZ9, Dayton and Franklin grown on neutral soil (control) and acid soil (pH 4.7; 13.6 mEq/kg exchangeable Al). (B) Root growth under 144 h of 5  $\mu$ M Al treatment. (C) Whole root Al concentration after 144 h Al treatment. (D) Citrate secretion from excised root tips exposed to 2 h of 5  $\mu$ M Al treatment. (E) *HvAACT1* gene expression in root tips under 2 h of 5  $\mu$ M Al treatment. (F) Gel electrophoresis of *HvAACT1* with 1-kb sequence insertion in the upstream of coding region of Dayton. Data are means  $\pm$  SE (n = 3). Different lower case letters indicate significant difference at  $P < 0.05$ .



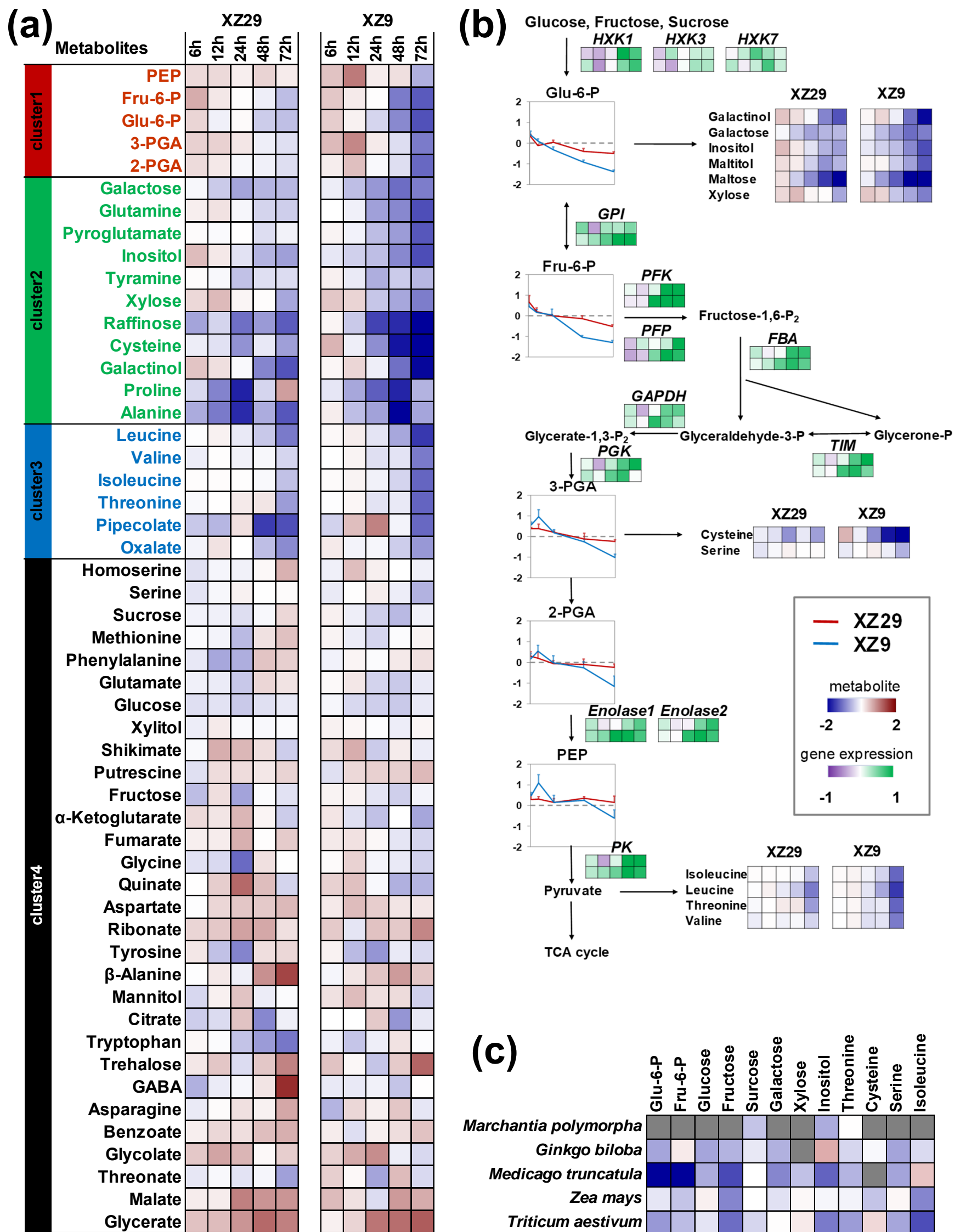


**Figure 4.** Primary metabolites in root tips of plants under Al treatments. (a) Heatmap of primary metabolites in root tips of XZ29 and XZ9 under Al treatment. Five blocks (for each metabolite and genotype) represent the changes of metabolite concentrations after 6, 12, 24, 48, and 72 h of 5  $\mu$ M Al treatments (from left to right) respectively. The color of block represents the change of metabolite concentrations, which is displayed as log<sub>2</sub> transformed ratio of metabolite concentration under Al treatment to metabolite concentration under control condition (control was sampled at each time point). Dark red (value=2) represents that metabolite concentration in treatment is four-fold as that in control, while dark blue (value=-2) represents that the metabolite concentration in treatment is 0.25-fold as that in control. Cluster analysis was performed using K-mean method by SPSS. Four biological replicates were used. (b) Temporal changes of metabolites and gene expressions in glycolytic pathway. In the line charts, y axis represents the log<sub>2</sub> transformed ratio of metabolite concentration under Al treatment to metabolite concentration in the control (control plant was also sampled at each time point), and x axis represents the time of Al treatment. In the heatmap of gene expressions, five blocks represent the relative gene expression after 0.5, 2, 6, 12 and 24 h of 5  $\mu$ M Al treatments. Green represents up-regulation and purple represents down-regulation. (c) Al-induced the change of primary metabolites in root tips of five plant species including *Marchantia polymorpha*, *Ginkgo biloba*, *Medicago truncatula*, *Zea mays* and *Triticum aestivum*. Gray block means that the metabolite was not detected in the sample.

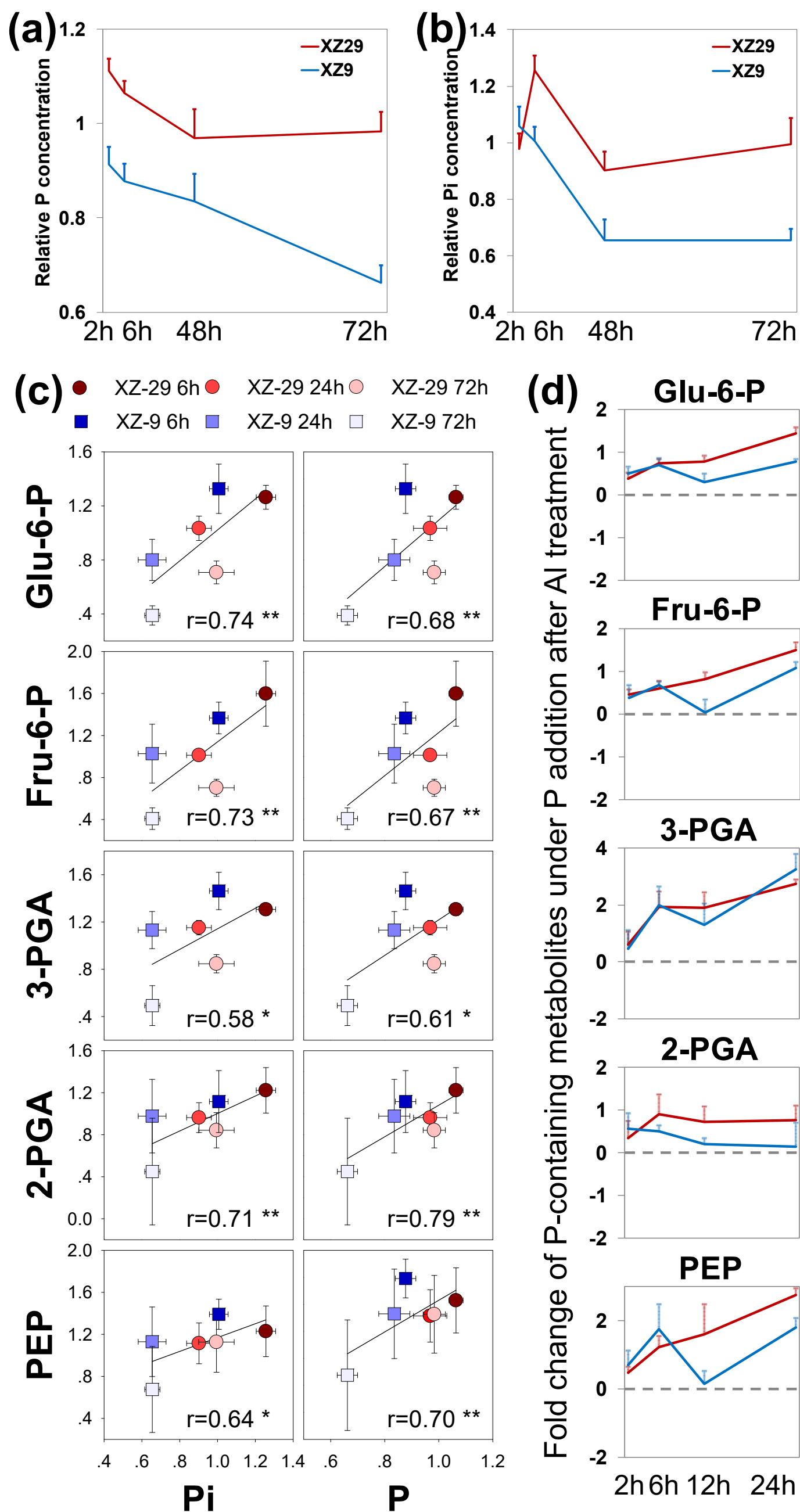


**Figure 5.** The effect of P and Pi on P-containing glycolytic intermediates under Al stress. (a, b) Relative P and Pi concentrations in root tips after 2, 6, 24, and 72 h Al treatments. (c) Correlation analysis between P-containing glycolytic intermediates and root tip P and Pi concentrations. The glycolytic intermediates, P and Pi concentrations under 6, 24, and 72 h of Al treatments were used. (d) Temporal changes of P-containing glycolytic intermediates in response to 2, 6, 12 and 24 h of P addition after 72 h Al treatment. Data are means  $\pm$  SE (n =3-4). \*P<0.05, \*\*P<0.01.

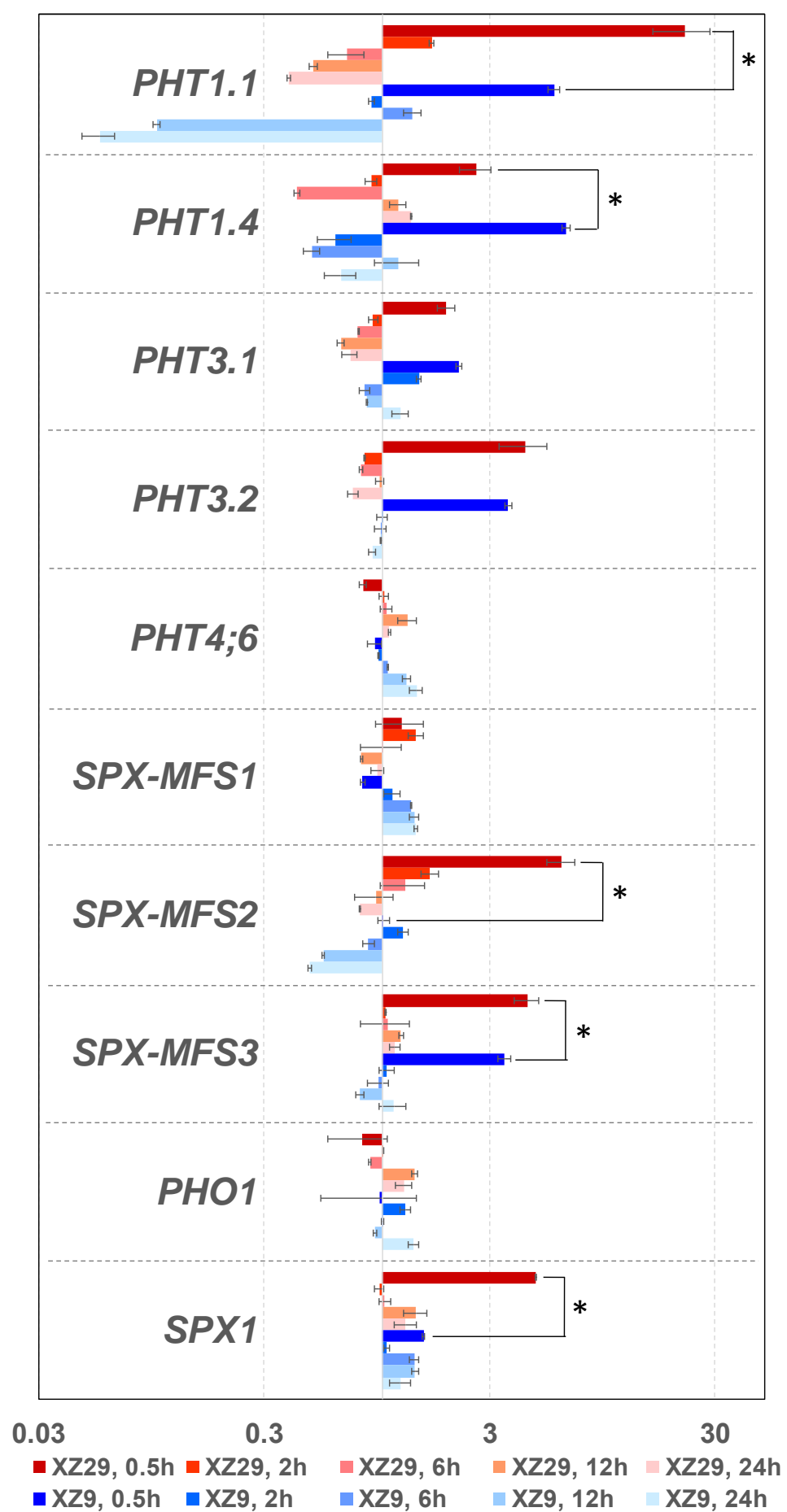


**Figure 6.** Effect of Al treatments on the expression of Pi transporter/signaling genes in XZ29 and XZ9. Gene expression of Pi transporters/signaling in root tips after 0.5, 2, 6, 12, and 24 h of 5  $\mu$ M Al treatments. Data are means  $\pm$  SE (n = 4 biological replicates). \* represents significant difference between genotypes at P<0.05

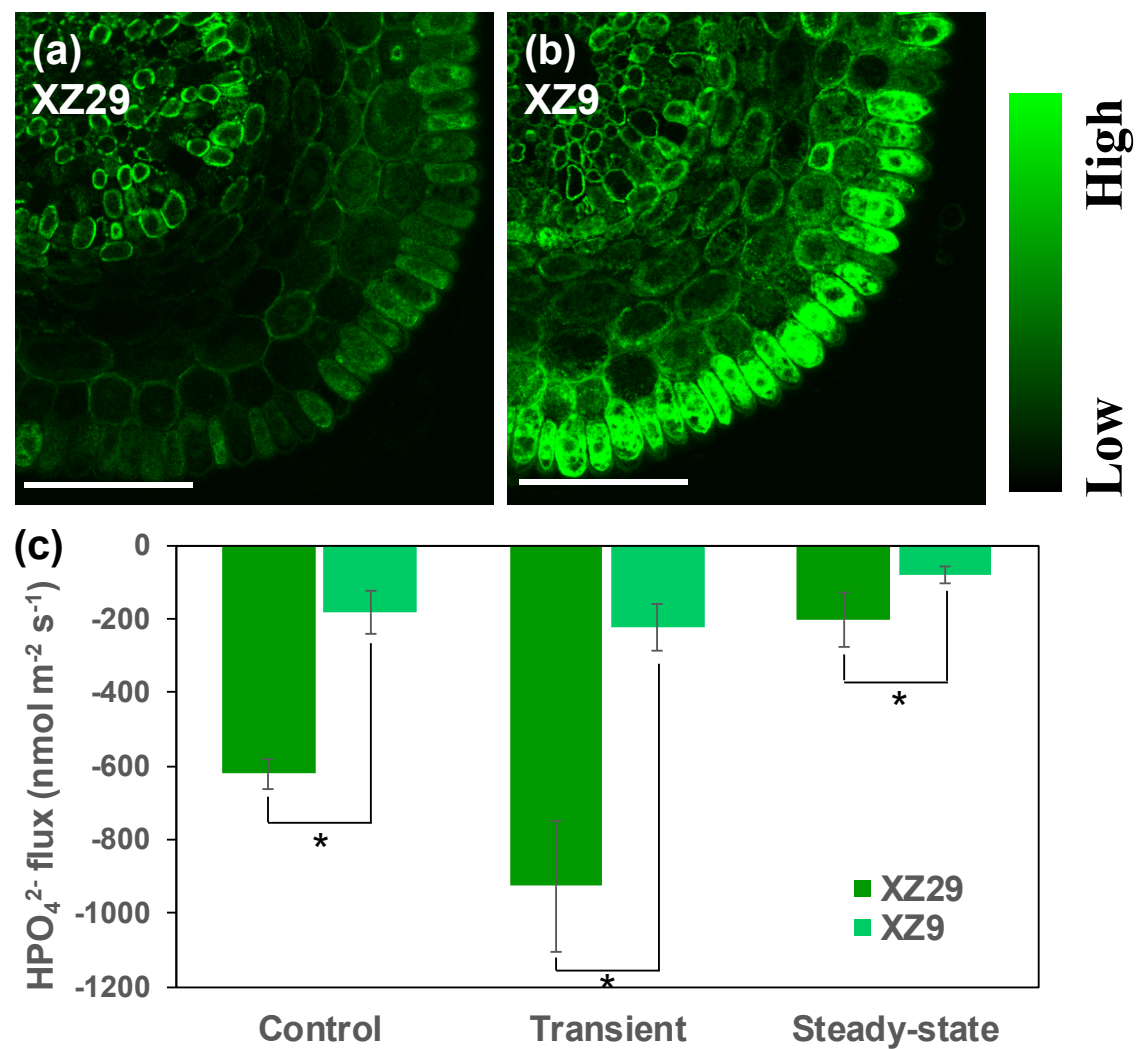


**Figure 7.** Al-morin fluorescence and Al-induced root  $\text{HPO}_4^{2-}$  flux in root elongation zone in XZ29 and XZ9. (a, b) Al-morin fluorescence imaging of Al distribution in the cross-sections of root elongation zone after 6 h Al treatment. A total of 6-8 replicates were performed for each genotype, and the representative images were shown. Scale bars: 50  $\mu\text{m}$ . (c) Al-induced root  $\text{HPO}_4^{2-}$  flux of XZ29 and XZ9. The  $\text{HPO}_4^{2-}$  flux was determined when plants (three-day-old seedling) incubated in MIFE basal solution (500  $\mu\text{M}$  KCl and 100  $\mu\text{M}$  CaCl<sub>2</sub> with pH 4.3). Average Al-induced net  $\text{HPO}_4^{2-}$  fluxes in the control (0-10 min), transient (11 to 15 min) and steady-state (30-40 min) were measured from elongation zone response to 25  $\mu\text{M}$  Al treatment. Influx (uptake) of the ions has a positive sign and efflux (release) has a negative sign. Data are means  $\pm$  SE (n=6-10 biological samples). \* represents significant difference at  $P < 0.05$ .

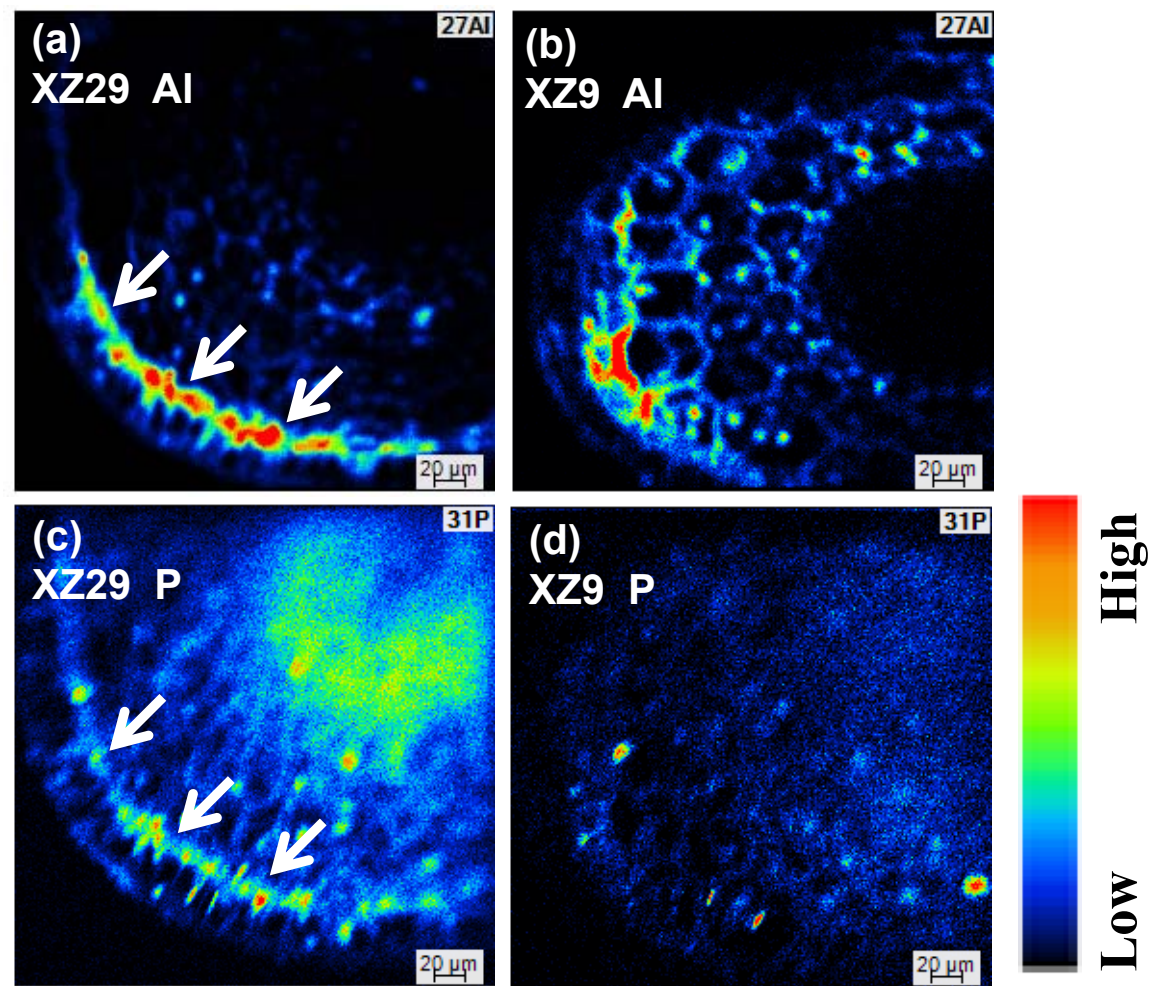


**Figure 8.** Secondary ion mass spectrometry (SIMS) of Al and P distribution in cross-sections of root mature zone in XZ29 and XZ9. Al and P distribution in root mature zone of XZ29 (a, c) and XZ9 (b, d) after 72 h of 5  $\mu$ M Al treatment. Shown are representative images (n=4-6). Scale bars: 50  $\mu$ m.



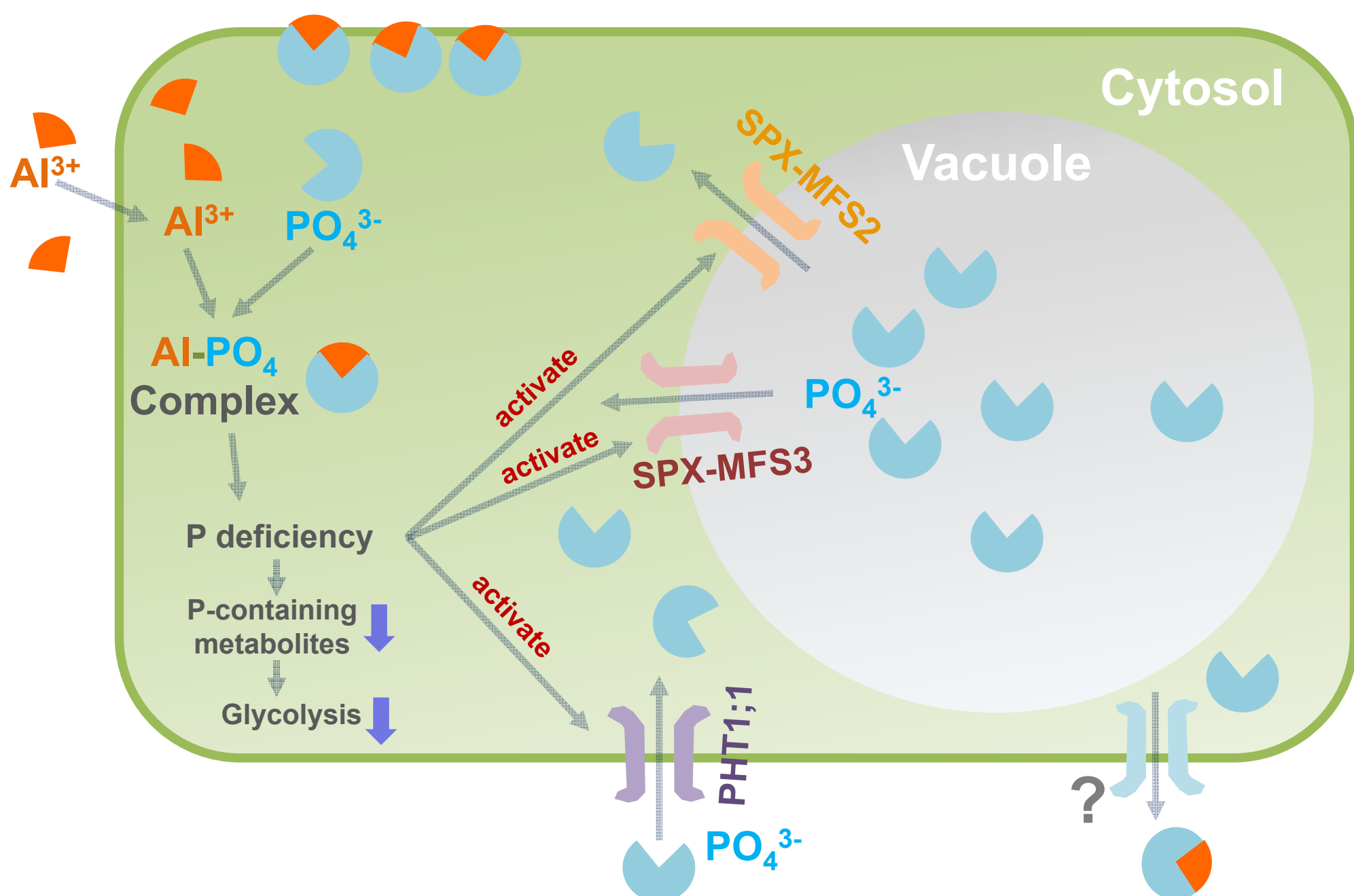


**Figure 9.** Putative schematic diagram of cellular P transport and metabolism in Tibetan wild barley XZ29 under Al stress.  $\text{Al}^{3+}$  enters into the cell, and binds with  $\text{PO}_4^{3-}$  to form Al-P complex. This decreased the cytosolic Pi level, resulting in reduction of P-containing glycolytic intermediates and inhibition of glycolysis. Cytosolic P deficiency activates Pi efflux from vacuole to cytosol probably mediated by the tonoplast Pi efflux transporters SPX-MFS2/3, to enhance the cytosolic Pi level. Immobilization of Al with P in the cell wall or apoplast is observed. Al treatment induces a transient Pi efflux from root to chelate the rhizosphere  $\text{Al}^{3+}$ . However, the transporter or ion channel is unknown.

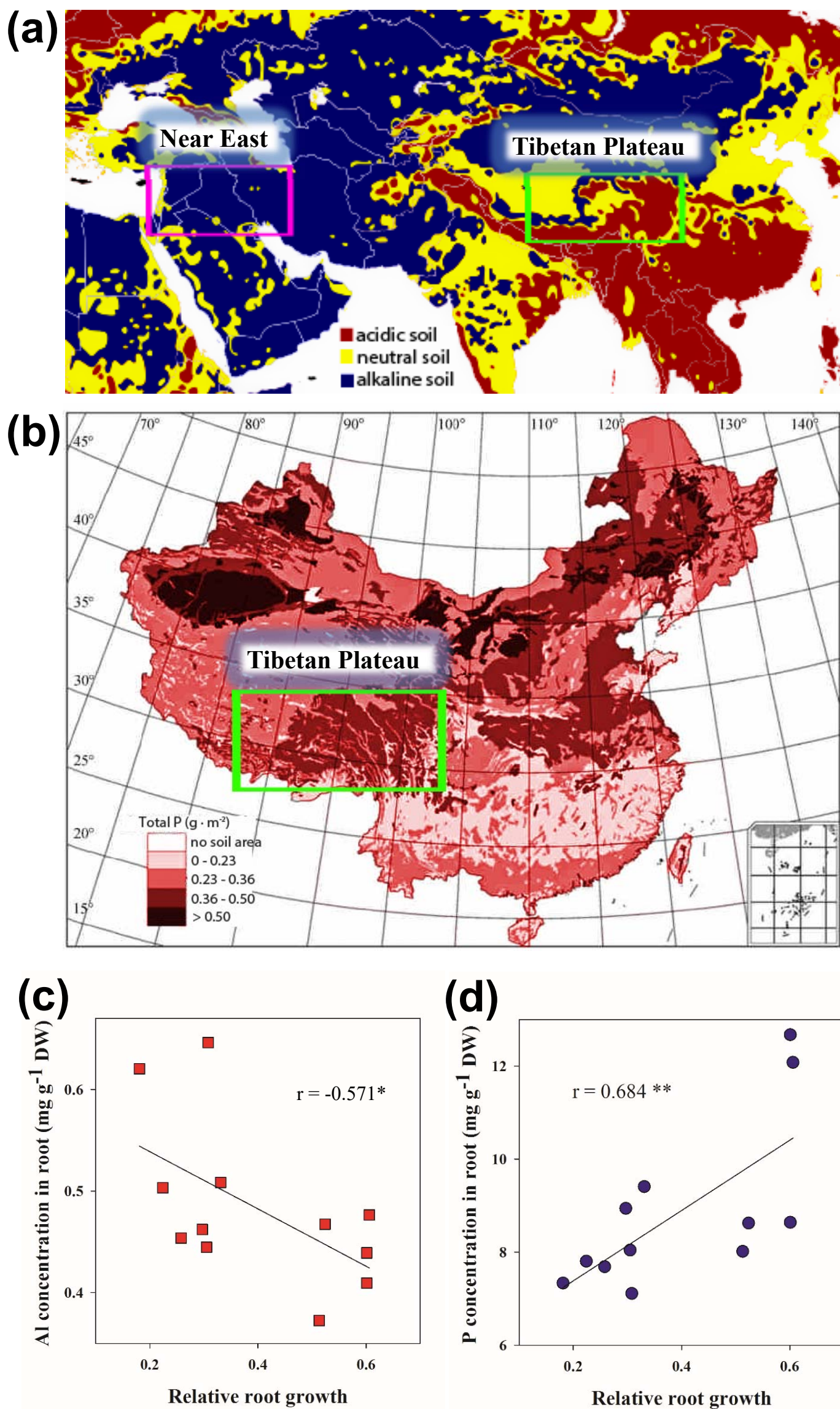


**Figure 10.** Linking soil acidity and total soil phosphorus (P) in centers of barley origin (Near East and Tibetan Plateau) to Al and P concentration in Tibetan wild barley under Al stress. (a) Southern and southeastern Tibetan plateau has acidic soil (green box) and Near East has alkaline soil (pink box). Source <http://nelson.wisc.edu/sage/data-and-models/atlas>. (b) P distribution in China. Southern and southeastern Tibetan plateau has high total soil P (green box) (Wang et al., 2008). (c, d) correlation analysis between relative root growth and Al and P content in 12 Tibetan wild barley accessions under Al stress. \* $P < 0.05$ , \*\* $P < 0.01$ .